# THE EFFECT OF NANO-REINFORCED FIBER/MATRIX INTERPHASE ON STRESSES IN STEEL FIBER COMPOSITES

Baris Sabuncuoglu*, Larissa Gorbatikh, Stepan V. Lomov

*Department of Metallurgy and Materials Engineering (MTM), KU Leuven, Kasteelpark Arenberg 44, B-3001 Heverlee, Belgium*
**baris.sabuncuoglu@mtm.kuleuven.be*

**Keywords:** Steel fibers, interfaces, nanoreinforcements, finite element

## Abstract

*Continuous steel fiber polymer composites are susceptible to SCs (SCs) under transverse loading. This is due to the high mismatch in elastic properties between steel fiber and polymer matrix. Nano-reinforcement of the fiber/matrix interphase can potentially reduce these SCs. In the present work two types of nano-modifications are investigated using finite element (FE) analysis: carbon nanotube (CNTs) forests and graphene based fiber coatings/sizings. Homogenized properties of the nano-reinforced interphase are first calculated using inclusion based and then implemented in the FE model. Results indicate that the presence of nano-reinforcements near the fiber interface increases radial SCs around the fiber as well as SCs in the direction of the applied load. The suppression is only observed for shear SCs in the case of grown CNTs.*

## 1. Introduction

The onset of damage in composites is characterized by the material properties of fiber and matrix. High stiffness mismatch between them would lead to high SCs near the fiber-matrix interface [1], and cause premature matrix cracking. Steel fiber composites are attractive in composite technology as they combine high stiffness together with high ductility [2]. One of the challenges of using steel fibers in composites is the stiffness contrast between the fibers and polymeric matrix due to high SCs [3]. In addition, steel fibers have a cross-sectional shape of an irregular polygon due their method of production [4] This additionally increases the SCs near sharp corners of the fiber [5,3]. One of the possible ways to suppress is to decrease the property mismatch by introducing an interphase between fiber and matrix with gradient properties.

The interphase can be created by introducing nano-scale reinforcements such as nanoparticles, nanotubes and nanoclays. These modifications affect mechanical properties of fiber-matrix interface and increase the overall performance of composite in terms of tensile strength [6], fracture toughness [7] and hardness [8]. The fiber-matrix interface created by these nanoreinforcements, has a stiffness value between the matrix and fiber stiffness [9-11]. Thus creation of such an interface can also be beneficial to reduce the SCs under transverse loading.

The objective of the present study is to evaluate the effect of nano-modified interphases on the SCs in steel fiber composites under transverse loading. Two different types of nano reinforced interphases are analyzed: with grown aligned CNTs and with graphene modified sizings (Figure 1). The elastic properties of the nano-reinforced interphase are first calculated using inclusion based homogenization approaches [12]. The study is performed using Abaqus finite element software with special subroutines to apply the contribution of stiffness of the nanoreinforcements and to extract stress results in the matrix.

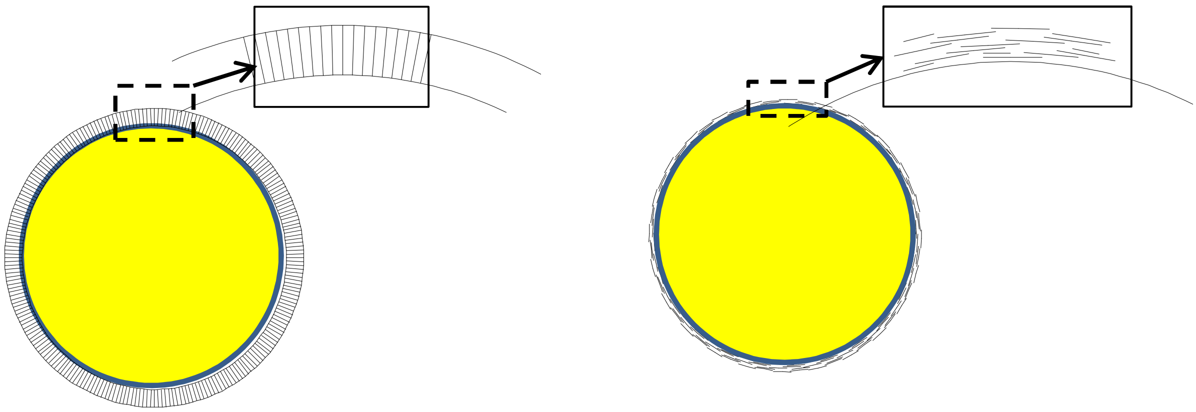

(a) (b)

**Figure 1.** Schematic representation of (a) straight CNTs grown on fiber surface and (b) graphene modified sizing/coating on fiber surface

## 2. Nano-reinforced interphase

The first nano-reinforcement type is a forest of aligned CNTs grown on fiber surface [13]. A CNT is a cylinder-like reinforcement. Its diameter and length are assumed to be 9 nm and 2 μm, respectively [14]. The CNT weight percentage is chosen as $5\%$, measured with respect to the weight of carbon fibers [15]. The second type of the considered interphase is the fiber sizing reinforced with graphene [16]. Graphene is a platelet-like morphology, meaning that they have a very thin but wide aspect ratio. Its sizing on the surface of carbon fibers can be done by electrophoretic deposition and subsequent thermal annealing [17]. In the present study, the volumetric ratio of graphene in the matrix is chosen to be 3%, which is the maximum value studied in [18]. The thickness of the graphene-reinforced layer is taken to be 1 μm.

Both nanoreinforcements have transversely isotropic elastic properties, which are provided in Table 1. The properties in the material directions 1 and 2 are the same. The stiffness of CNT in the direction 3 is much higher than in the other two directions whereas for graphene it is much lower . The longitudinal modulus of CNT is assumed to be 300 GPa. As it is very difficult to determine the transverse properties, these are taken as the same as carbon fibers used in industry[19].The in-plane properties ($E_1$ and $\nu_{12}$) of graphene sheets are obtained from [20, 21]. The transverse properties are taken from [22]. The empty values in the table can be calculated with the use of the other values mentioned in the table.

| | CNT | Graphene Platelet |
|---|---|---|

| | 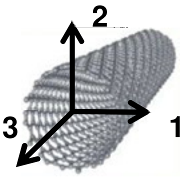  | 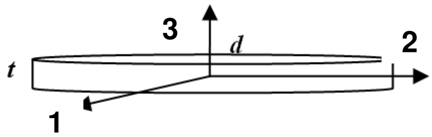  |
|---|---|---|
| $E_1$ (GPa) | 10.3 | 500 |
| $E_3$ (GPa) | 300 | 39.5 |
| $G_{13}$(GPa) | 27.9 | 26.8 |
| $G_{12}$(GPa) | 3.8 | |
| $\nu_{31}$ | 0.3 | |
| $\nu_{12}$ | | 0.23 |
| $\nu_{13}$ | | 0.006 |

**Table 1.** Material properties of CNTs and graphene platelets used in the study.

## 3. Models and boundary conditions

Constructed models for two cross-section types are presented in Figure 4 with the boundary conditions. Displacement ($u_0$) is applied along the *x*-direction to obtain a constant strain of $\varepsilon_0$=0.2% by taking in the account the dimensions of the model. Additional interface regions near the fibers are introduced to facilitate assessment of interphase stresses. Models are constructed with the fiber diameter 30 μm for steel fibers and two fiber volume fractions 0.4 and 0.6 [3] which are generally the upper and lower limits used in composites. The model with hexagonal fiber cross-sections is constructed with dimensions that would lead to the same area as in the case of circular fiber cross-sections. In order to prevent SCs at the fiber corners, a slight fillet of 2 μm is introduced. The latter was estimated from microscopy images of the composite cross-sections [23]. Material properties of fiber and matrix are given in Table 2. Young's modulus of steel fibers is determined from the tensile tests performed in NV Bekaert [24]. Properties of epoxy are determined from [25].

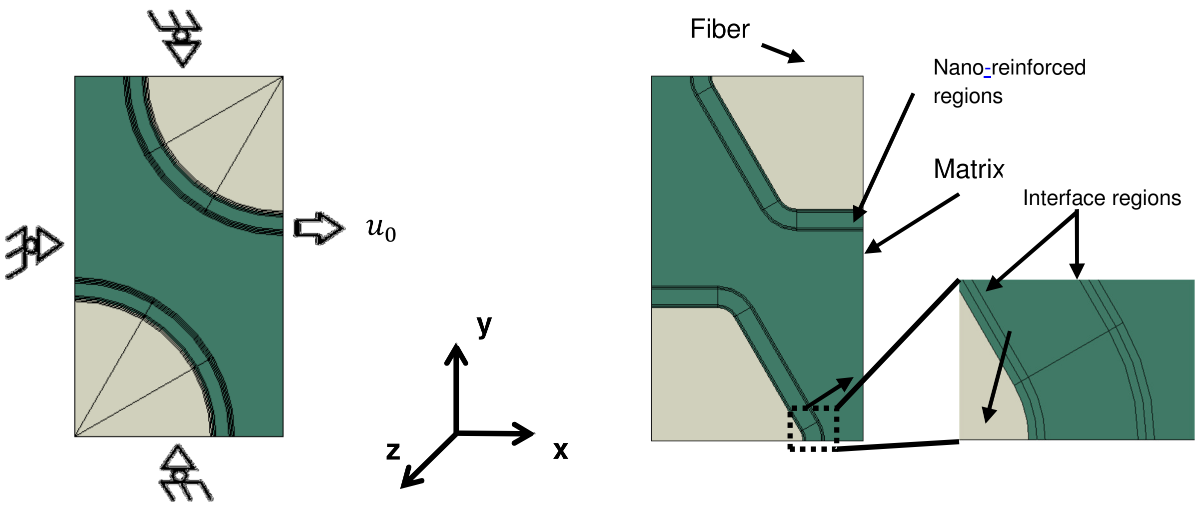

(a) (b)

**Figure 2.** Models and boundary conditions for fibers with (a) circular; (b) hexagonal cross-sections.

| Steel | Epoxy |
|---|---|
| $E$=193 GPa | $E$=3 GPa |
| $\upsilon$=0.3 | $\upsilon$=0.4 |

**Table 2**. Material properties of steel and epoxy ($E$: Young's modulus, $\upsilon$, Poisson's ratio)

## 4. Homogenized properties of the interphase

The homogenized stiffness of the nano-reinforced interphases is calculated using inclusion based Mori-Tanaka approach. It was then assigned to the elements in the FE model with respect to the location of integration points using UMAT subroutine in Abaqus®. The calculations are based on the volumetric ratios of CNT ($\upsilon\_CNT$) or graphene ($\upsilon\_g$) in the matrix and their orientation which is calculated based on the data given in section 2. The volumetric ratio of CNTs and graphene platelets in the fiber/matrix interphase in relation to the volume of the interphase is shown in Figure 3. *v_cnt* decreases when the location distance from the fiber surface increases due to the radial orientation of CNTs.

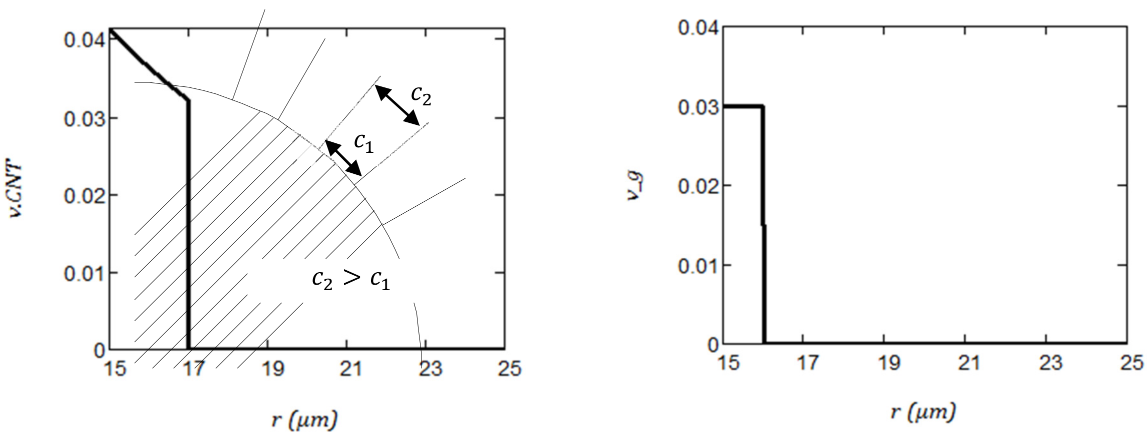


(a) (b)

**Figure 3.** Variation of the volumetric ratio of nano-reinforcements as a function of the distance to the fiber surface for the case of (a) CNTs; (b) graphene.

The third model assumes that graphene platelets are evenly distributed all over the matrix. This is considered in order to investigate the effect of graphene localization. The volumetric ratio of graphene in the case of the fiber sizing is scaled with the volume of the matrix to represent the same amount of platelets in the matrix. Homogenized elastic properties of the matrix are calculated according to [26].

Stresses of interest are the radial ($\sigma_{rr}$) and shear ($\sigma_{r\theta}$) stress components (in the polar coordinate system introduced in the fiber center). They control the onset of debonding at the fiber/matrix interface. The stress component $\sigma_x$ (aligned with the load direction) is also calculated to determine the stress distribution along from fiber-matrix interphase to the edge of the model. The calculated components are normalized by the average stress ($\sigma_{x\_ave}$) applied to the model. Note that even with the same applied average strain, the average stress will be different for different models due to differences in the homogenized stiffness.

## 5. Results

The variation of $\sigma_x$ concentrations $\left(Kx = \frac{\sigma_x}{\sigma_{x_{ave}}}\right)$ through the matrix, the radial ($Kr = \frac{\sigma_{rr}}{\sigma_{x_{ave}}}$) and shear ($Kr\theta = \frac{\sigma_{r\theta}}{\sigma_{x_{ave}}}$) SCs along the fiber-matrix interface for both nano-reinforced interphases and the two fiber volume fractions are shown in Figure 4 along with the case of no nano-modified interphase. Depicted in Figure 4a and b, $L$ represents the distance from fiber edge to the model edge.

For all nano-reinforced interphases, the stress concentration $Kx$ values increased in contrast to expectations. The effect is more pronounced in the case of grown CNTs . CNTs are aligned perpendicular to the fiber surface. Thus, the direction of the highest stiffness is along the radial direction to the fibers. In the case of graphene reinforced sizing, this direction is the direction of lowest stiffness as they are aligned in tangential directions. When the graphene platelets are distributed randomly in the matrix instead of being localized near the fiber, it results in lower SCs even compared to the reference case (without nanoreinforcements). Similar results can be observed for radial SCs.

The shear SCs are found to be the lowest in the model with CNTs. When CNTs are aligned in the radial direction, the stiffness at the interface along the tangential direction to the fiber surface is much lower compared to the one in the radial direction. Thus, most of the applied load is carried by their longitudinal direction.

The case of hexagonal fiber cross-section is studied for aligned CNT forests for $vf$ = 0.4. Normal SCs ($Kn = \frac{\sigma_n}{\sigma_{x_{ave}}}$ ) is calculated with the stress component in the fiber-matrix interface, perpendicular to the surface of the fiber at each location of interface nodes (Figure 5). Apparently, the effect of nanoreinforcements is more pronounced in the case of polygonal cross-sections.

## 6. Conclusion

The effect of nano-reinforced interphases on transverse SCs in unidirectional steel fiber composites under transverse loading was investigated. According to the results, the introduction of such interphases increases normal SCs against expectations. The level of the concentrations increases with fiber volume fraction of nano-reinforcements in the matrix. They are also higher for fibers with polygonal cross-sections. On the other hand, shear SCs decrease in the case of CNTs, This may provide some benefits for the structural integrity of adhesives at the fiber-matrix interface. In the case of fibers with hexagonal cross-sections, much higher stresses are observed at the locations where SCs coincide with the corners of the hexagon.

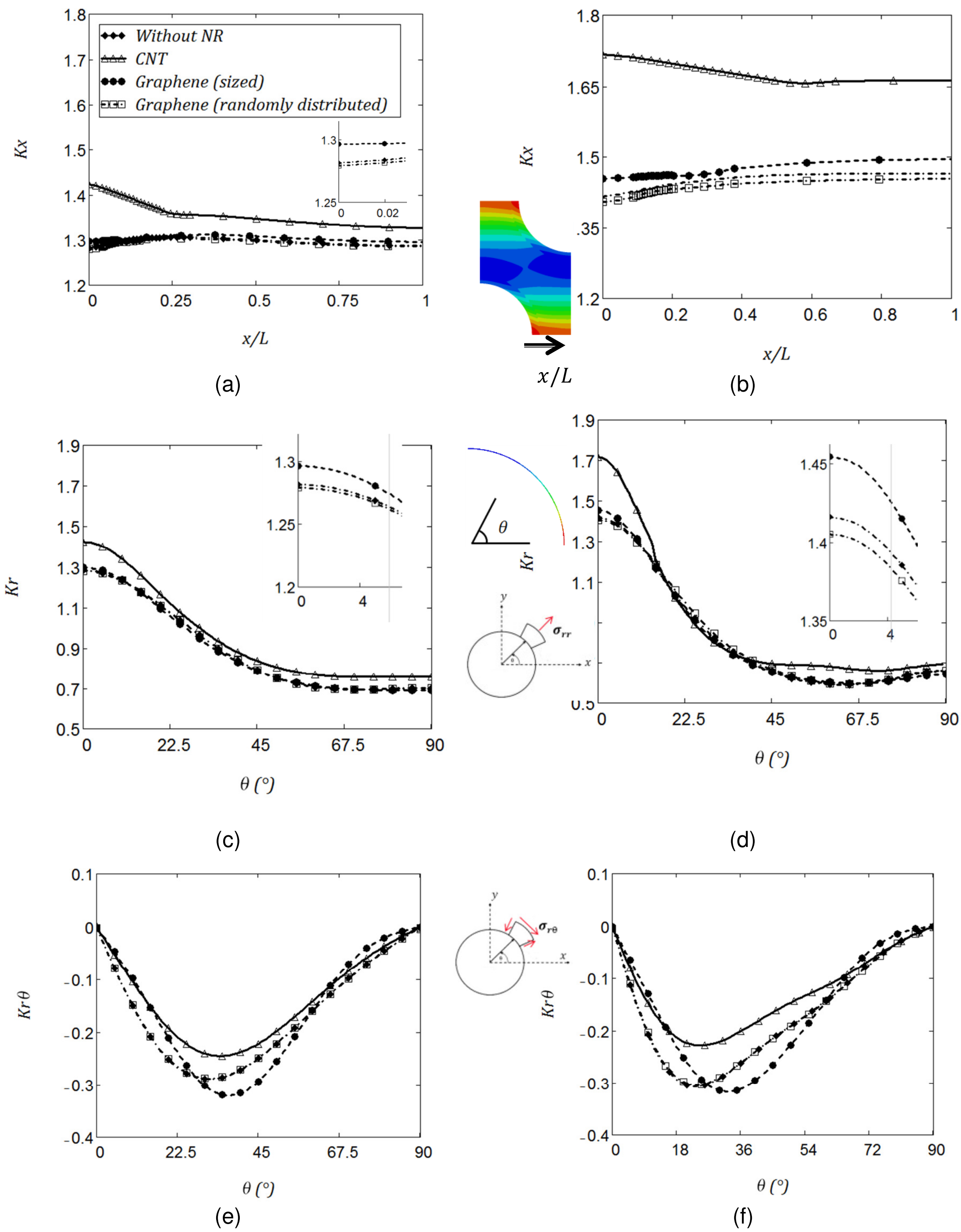


**Figure 4.** Effect of nano-reinforced interphases: (a), (b) horizontal SCs along the fiber-matrix interface for vf = 0.4 and vf = 0.6, respectively; (c), (d) radial SCs along the fiber-matrix interface for vf = 0.4 and vf = 0.6, respectively; (e), (f) shear SCs along the fiber-matrix interface for vf = 0.4 and vf = 0.6, respectively (*NR*: nanoreinforcements)

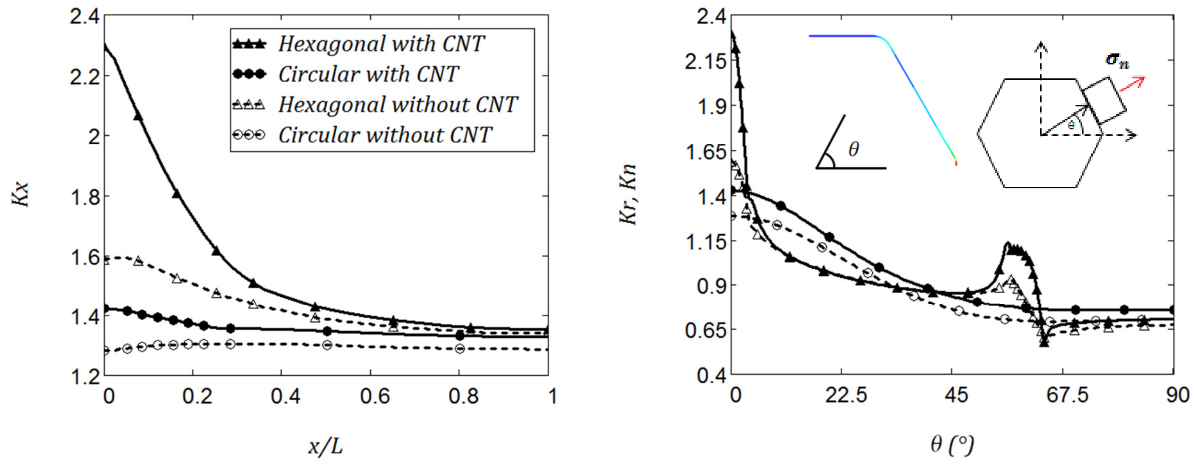


(a) (b)

**Figure 5**. Effect of nanoreinforcements: (a) Horizontal SCs towards the inside of the matrix; (b) radial and normal SCs in fiber-matrix matrix interface for $vf$ = 0.4

## Acknowledgement

The work reported here was funded by SIM and IWT (Flanders) in the framework of NANOFORCE program and SBO-2 project “Multi-level modeling of nano-engineered hybrids”.

## References


[1] A.M. Skudra and B.M. Blue. *Structural Theory of Reinforced Plastics (in Russian),* Riga: Zinatne, Latvia, 1978

[2] M.G. Callens, L. Gorbatikh, E. Bertels, *et al.* Ductile steel fiber/epoxy composites with modified adhesion, *International Conference on Composite Materials (ICCM)*, Montréal, Canada, 2013.

[3] B.Sabuncuoglu, S. Orlova, L.Gorbatikh, S. Lomov, I. Verpoest, Micro-scale finite element analysis of SCs in steel fiber composites under transverse loading, *accepted to be published in Journal of Composite Materials*, 2014

[4] S. De Bondt, Decrop, J.' US 7,166,174 B2, US, 2007.

[5] J.P. Xie, A.Q. Wang, W.Y. Wang, *et al.* Stress field numerical simulation of the inclusions in large rudder arm steel casting, *Advanced Materials Research,* 311-313: 906-909, 2011.

[6] M.W. Ho, C.K. Lam, K. Lau, *et al.* Mechanical properties of epoxy-based composites using nanoclays. *Composite Structures*, 75: 415-421, 2006.

[7] A. Warrier, A. Godara, O. Rochez, *et al.* The effect of adding carbon nanotubes to glass/epoxy composites in the fibre sizing and/or the matrix. *Composites Part A,* 41: 532-538, 2010.

[8] F. Heydari, A. Maghsoudipour, Z. Hamnabard and S. Farhangdoust. Mechanical properties and microstructure characterization of zirconia nanoparticles glass composites for SOFC sealant. *Materials Science and Engineering A*, 552: 119-124, 2012.

[9] H. Qian, G. Kalinka, K.L. Chan, *et al.* Mapping local microstructure and mechanical performance around carbonnanotube grafted silica fibres: methodologies of hierarchical composites, *Nanoscale,* 3:4759-4767, 2011.

[10] G. Chatzigeorgiou, Y. Efendiev, D.C. Lagoudas, Homogenization of aligned fuzzy fiber composites, *International Journal of Solids and Structures*, 48:2668-2680, 2011.

[11] S.I. Kundalwal and M.C. Ray. Effective properties of novel continuous fuzzy-fiber reinforced composite using the method of cells and finite element method. *European Journal of Mechanics A/Solids*, 36: 191 – 203, 2012.

[12] T. Mura. *Micromechanics of Defects in Solids (Second Edition)* Kluwer Academic Publishers, Dordrecht, Netherlands, 1991.

[13] Lomov, S.V., S. Wicks, L. Gorbatikh, I. Verpoest, and B.L. Wardle, Compressibility of nanofiber-grafted alumina fabric and yarns: Aligned carbon nanotube forests. *Composites Science and Technology*, 2014. 90: 57-66.

[14] V. Romanov, S.V. Lomov, L. Gorbatikh and I. Verpoest. A novel approach to modelling of fiber-reinforced composites with carbon nanotubes. In *19th International Conference on Composite Materials (ICCM19)*. Montreal, Canada, 2013.

[15] E.J. Garcia, A.J. Hart, and B.L. Wardle, Long carbon nanotubes grown on the surface of fibers for hybrid composites. *AIAA Journal*, 46(6): 1405-1412, 2008.

[16] R. Sengupta. A review on the mechanical and electrical properties of prephite reinforced polymer composites. *Progress in Polymer Science*, 36: 638-670, 2011.

[17] S.Y. Huang, G.P. Wu, C.M. Chen *et al.*. Electrophoretic deposition and thermal annealing of a graphene oxide film on carbon fiber surfaces, *Carbon,* 52: 605-620, 2013.

[18] J.F. Zou, Z.Z. Yu, Y.X. Pan *et al.,* Conductive mechanism of polymer/graphite conducting composites with low percolation threshold, *Journal of Polymer Science B Polymer Physics*, 40: 954-963, 2002.

[19] A.Kelly, C. Zweben. Comprehensive Composite Materials, Vol. 1: Elsevier , 2000.

[20] Home Page of Graphenea, http://www.graphenea.com/pages/graphene-properties, last accessed 26/02.2004.

[21] P. Zhao and G. Shi. Study of Poisson's Ratios and single walled carbon nanotubes based on an improved molecular structural mechanics model. *CMC –Tech Science Press*, 22: 147-168, 2011.

[22] J. Cho, J.J. Luo, I.M. Daniel. Mechanical characterization of graphite/epoxy nanocomposites, *Composites Science and Technology,* 67: 2399–2407, 2007.

[23] M.G. Callens, L. Gorbatikh, I. Verpoest. Ductile steel fibre composites with brittle and ductile matrices, *Composites Part A – Applied Science and Manufacturing*, http://dx.doi.org/10.1016/j.compositesa.2014.02.006.

[24] NV Bekaert company website, http://www.bekaert.com/ (accessed 20/03/2014).

[25] F.A. Leckie, D.J. Bello. *Strength and Stiffness of Engineering Systems*, Springer Science and Business Media, New York, USA, 2009

[26] R.M. Christensen, *Mechanics of Composite Materials (Dover Edition)*, John Wiley & Sons, New York, USA, 2005